

Supporting Information

A two-dimensional zeolitic imidazolate framework loaded with an acrylate-substituted oxoiron cluster as efficient electrocatalysts for the oxygen evolution reaction

Zhuojie Xiao^a, Feng Xu^{a,*}

^a China State Key Laboratory for Chemo/Biosensing and Chemometrics, College of Chemistry & Chemical Engineering, Hunan University, Changsha, 410082, P. R. China

* Corresponding author.

E-mail address: feng_xu@hnu.edu.cn (Feng Xu)

Materials and Methods:

All of the reactants were reagent grade and used as purchased. Powder X-ray diffraction (PXRD) patterns were collected at room temperature on a Bruker D8 Advance. IR spectra were measured on PerkinElmer Spectrum 100 FT-IR spectrometer. X-ray photoelectron spectroscopy (XPS) were measured by Shimadzu AXIS SUPRA⁺. Scanning electron microscopy (SEM) and energy-dispersive X-ray spectrometry (EDS) mapping were measured by JSM-7610Fplus and ULTIM MAX 40. Transmission electron microscopy(TEM) and energy-dispersive X-ray spectrometry (EDS) mapping were measured by Titan G260-300 and SUPER EDX. N₂ adsorption desorption were measured by JW-BK200C.

TOF for OER

The total number of oxygen turnovers is calculated by using the following eq.

$$= j \frac{mA}{cm^2} \times \frac{\frac{1C}{s}}{1000 mA} \times \frac{1mol e^-}{96485 C} \times \frac{1mol O_2}{4 mol e^-} \times \frac{6.02 \times 10^{23} mol O_2}{1mol O_2} \times 1.56$$

$$= j \times 1.56 \times 10^{15} \frac{O_2 / s}{cm^2}$$

Accordingly, the density of active sites for OER based on the Co and Fe is calculated as eq.:

$$\left(\frac{27.6}{58.9} + \frac{7.42}{55.9} \right) \times \frac{1mmol}{100 mg} \times 0.57 \frac{mg}{cm^2} \times 6.022 \times 10^{20} \frac{sites}{mol}$$

$$= 2.06 \times 10^{18} sites cm^{-2}$$

For example, TOF of the catalyst for OER at an overpotential of 312 mV ($j = 10$ mA/cm²) is calculated as:

$$TOF = \frac{10 \times 1.56 \times 10^{15} \frac{O_2 / s}{cm^2}}{2.06 \times 10^{18} sites cm^{-2}} = 0.016 s^{-1}$$

Electrochemically active surface area

The electrochemically active surface area (ECSA) of the prepared catalyst was investigated through calculating the double-layer capacitance (C_{dl}) by recording the CV curve with the non-Faradic region with different scan rate of 20-120 mV s⁻¹. The slope of capacitive current ($\Delta j = j_{\text{anode}} - j_{\text{cathode}}$) vs scan rate was double the value of C_{dl} . The double-layer capacitance (C_{dl}) is directly proportional to ECSA, as given below.[1]

$$ECSA = \frac{C_{dl}}{C_s}$$

ECSA = Electrochemical active surface area (ECSA)

C_{dl} = Double layer capacitance

C_s = Specific capacitance (0.040 mF cm⁻²)

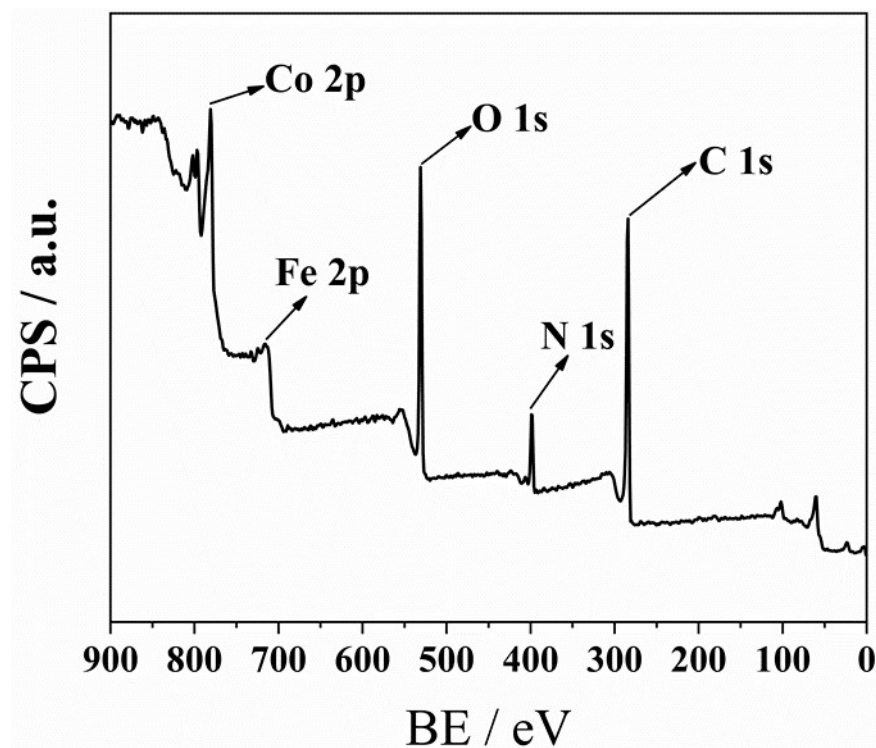


Fig. S1. XPS survey scan spectra of ZIF-L@Fe₂₈

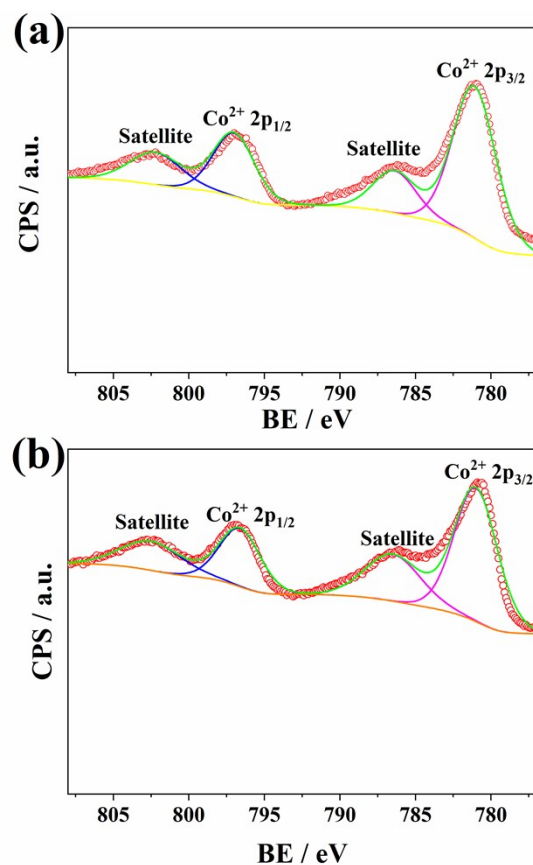


Fig. S2. Deconvolutions of XPS Co 2p core-level regions for (a) ZIF-L and (b) ZIF-L@Fe₂₈

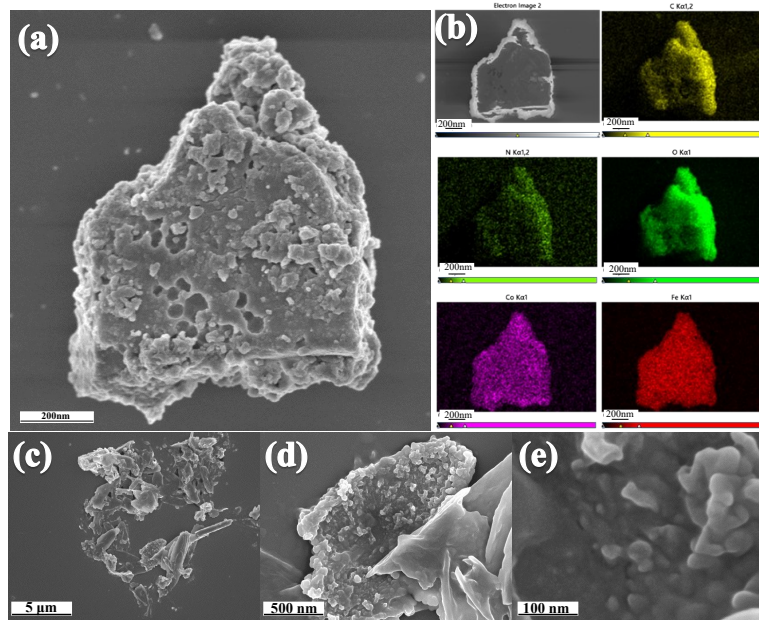


Fig. S3. SEM and corresponding EDS mapping images of ZIF-L@Fe₂₈ (160 mg)

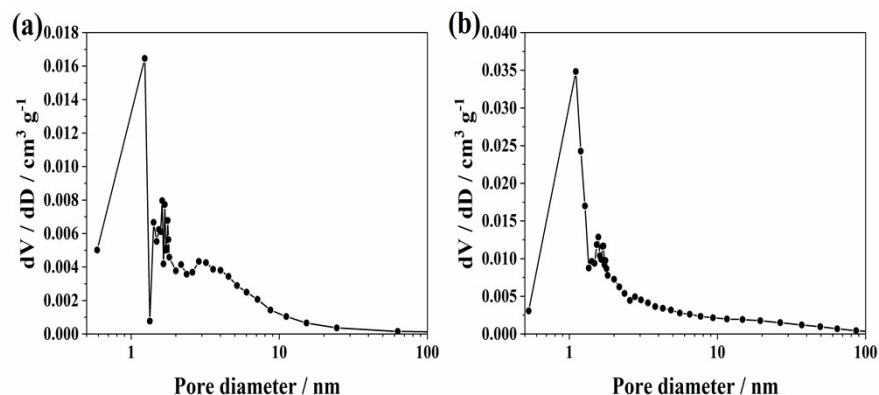


Figure S4. The pore size distribution curves of (a) ZIF-L and (b) ZIF-L@Fe₂₈.

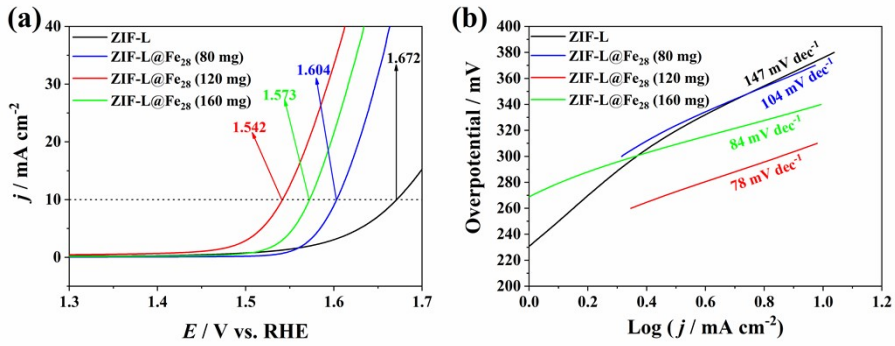


Fig. S5. LSV polarization curves of ZIF-L, ZIF-L@ Fe_{28} (80mg), ZIF-L@ Fe_{28} (120mg) and ZIF-L@ Fe_{28} (160mg). (b) The corresponding Tafel plots of the catalysts.

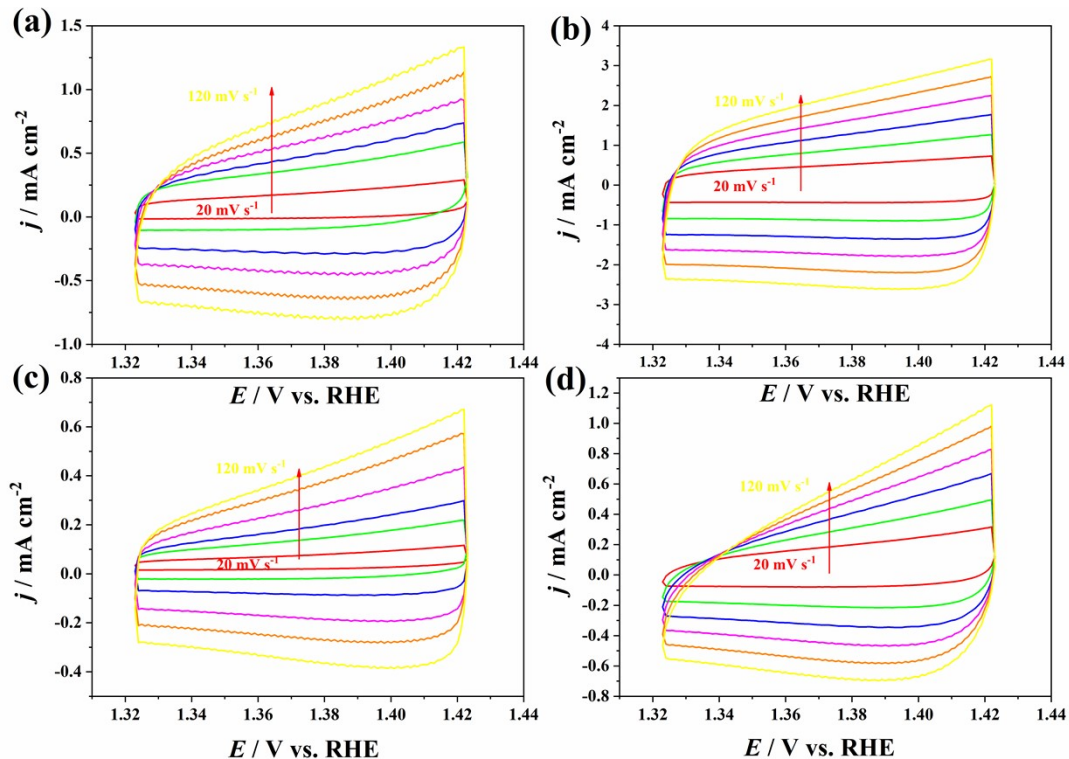


Fig. S6. CVs in a non-faradic current region (1.423-1.323 V) at different scan rates (20 to 120 mV/s) of (a) ZIF-L, (b) ZIF-L@ Fe_{28} (120 mg), (c) ZIF-67, and (d) ZIF-67@ Fe_{28} (120 mg) in 1.0 mol/L KOH solution.

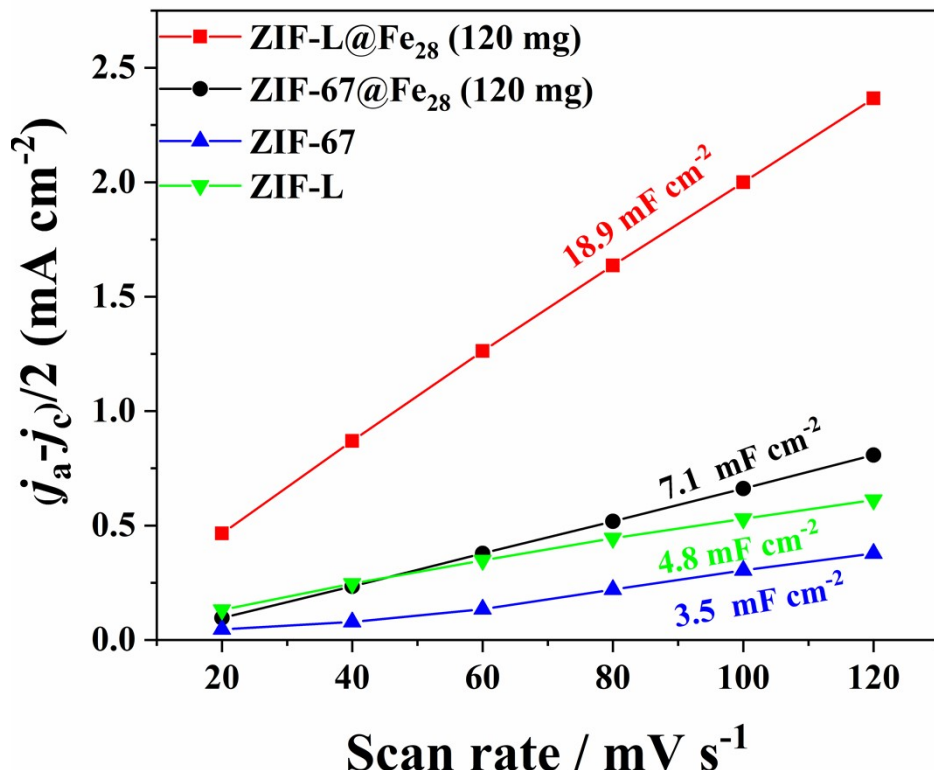


Fig. S7. $(j_a - j_c)/2$ plotted against scan rates of ZIF-L, ZIF-L@Fe₂₈ (120 mg), ZIF-67 and ZIF-67@Fe₂₈ (120 mg)

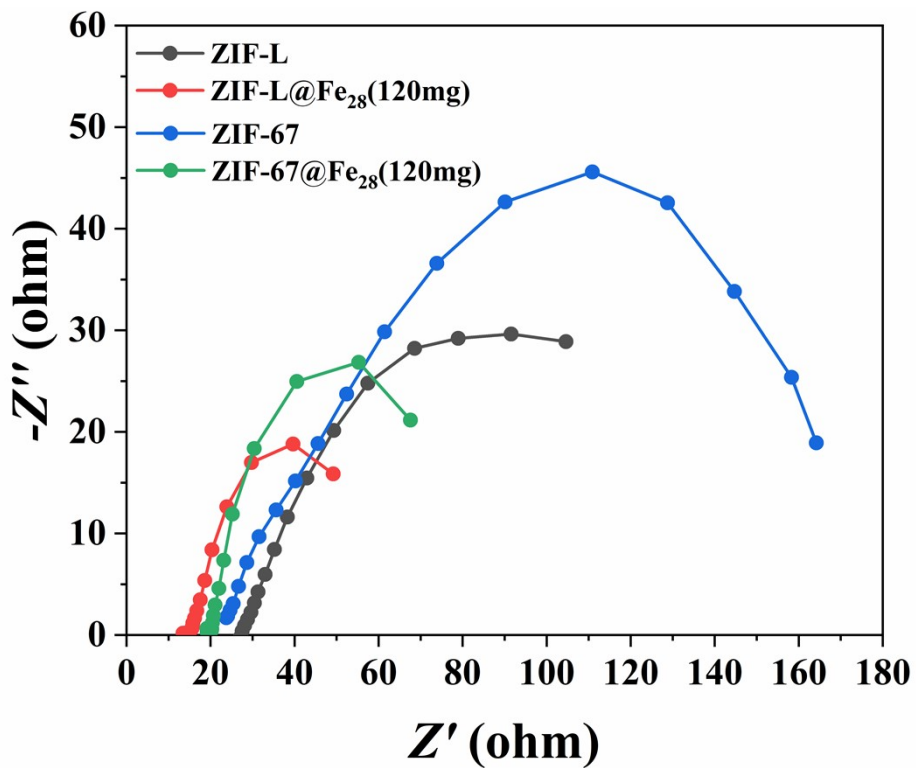


Fig. S8. EIS Nyquist plots of ZIF-L, ZIF-L@Fe₂₈(120mg), ZIF-67, ZIF-67@Fe₂₈(120mg) under a potential of 1.56V.

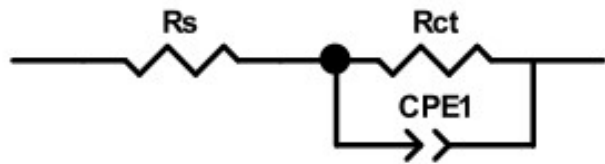


Figure S9. Equivalent circuit for the EIS data simulation, where R_s , R_{ct} and $CPE1$ represent the solution resistance, charge transfer resistance and constant-phase element, respectively. The fitting results are shown in Table S2.

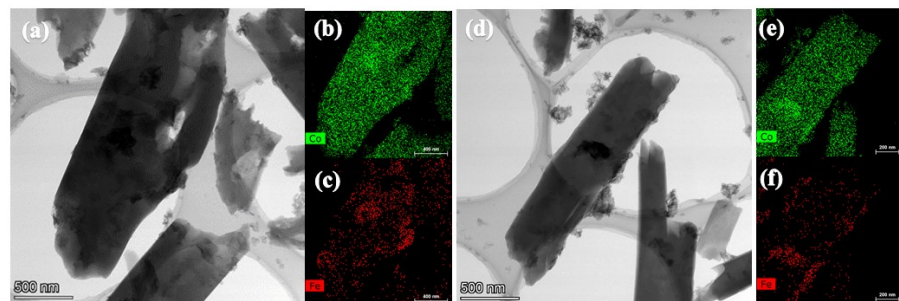


Figure S10. TEM images of ZIF-L@Fe₂₈ (120 mg) a,b,c) before and d,e,f) after OER tests.

Table S1. Elemental analysis data of iron and copper in {Fe₂₈}.

	Cu	Fe	molar ratio (Cu/Fe)
Fe ₂₈	1.142%	25.36%	1.1:28
ZIF-L@Fe ₂₈ (120 mg)	0.118%	7.421	0.39:28

Table S2. Surface element composition (XPS) of the ZIF-L and the ZIF-L@Fe₂₈ composite.

Catalysts	C	O	N	Co	Fe
ZIF-L	57.63	15.77	20.57	6.03	0
ZIF-L@Fe ₂₈	49.71	27.93	10.49	8.39	3.45

Table S3. The EIS fitting results of samples by fitting with the proposed equivalent circuit.

	ZIF-L	ZIF-L@Fe ₂₈ (120mg)	ZIF-67	ZIF-67@Fe ₂₈ (120mg)
R _s (Ω)	27.5	16.3	22.6	20.3
R _{ct} (Ω)	118.0	46.7	175.7	61.8

Table S4. The C_{dl}, ECSA, TOF and mass activity of ZIF-L, ZIF-L@Fe₂₈(120mg), ZIF-67, ZIF-67@Fe₂₈(120mg)

	ZIF-L	ZIF-L@Fe ₂₈ (120mg)	ZIF-67	ZIF-67@Fe ₂₈ (120mg)
C _{dl} (mF cm ⁻²)	4.8	18.9	3.5	7.1
ECSA (m ² g ⁻¹)	120.0	472.5	87.5	177.5
TOF (s ⁻¹)	0.002	0.016	0.0014	0.005
mass activity (A mg ⁻¹)	0.0025	0.02	0.0018	0.006

Table S5. Comparison of OER activities for the reported MOF-based catalysts.

Catalysts	Electrolyte	Overpotential (mV)	Tafel slope (mV dec ⁻¹)	Reference
Yolk/shell ZIF-67@POM	1.0 M KOH	287(10 mA cm ⁻²)	58	2
ZIF-8@ZIF-67@POM	1.0 M KOH	490(10 mA cm ⁻²)	88	3
PBA@POM	1.0 M KOH	440(10 mA cm ⁻²)	23	4
SiW ₉ Co ₃ [h]@ZIF-67	0.1 M KOH	420(10 mA cm ⁻²)	94	5
Mo _x Co _x C@C	1.0 M KOH	295(10 mA cm ⁻²)	39	6
Co-Mo ₂ C@NC	Phosphate buffer (pH =7)	440(10 mA cm ⁻²)	156	7
Fe/Ni _{2.4} /Co _{0.4} -MIL-53	1.0 M KOH	219(10 mA cm ⁻²)	54	8
Quasi-ZIF-67-350	1.0 M KOH	286(10 mA cm ⁻²)	84	9
WS ₂ /Co _{1-x} S/N	1.0 M KOH	365(10 mA cm ⁻²)	64	10
Co ₃ O ₄ /CoMoO ₄ nanocages	1.0 M KOH	318(10 mA cm ⁻²)	63	11
ZIF-L@Fe ₂₈	1.0 M KOH	312(10 mA cm ⁻²)	78	This work

References

- [1] M. Yu, G. Moon, E. Bill, et al., ACS Appl. Energy Mater. 2 (2019) 1199-1209.
- [2] Q.Y Li, L. Zhang, Y.X Xu, et al., ACS Sustain. Chem. Eng. 7 (2019) 5027-5033.
- [3] Y Wang, Y Wang, Li Zhang, et al., Inorg. Chem. Front. 6 (2019) 2514-2520.
- [4] Y. Wang, Y. Wang, L. Zhang, et al., Chem.-Asian J. 14 (2019) 2790-2795.
- [5] V.K. Abdelkader-Fernández, D.M. Fernandes, S.S. Balula, et al., J. Mater. Chem. A. 8 (2020) 13509-13521.
- [6] C. Chen, A. Wu, H. Yan, et al., Chem. Sci. 9 (2018) 4746-4755.
- [7] M. Wang, S. Dipazir, P. Lu, et al., J. Colloid Interface Sci. 532 (2018) 774-781.
- [8] F. L Li, Q. Shao, X Huang, et al., Angew. Chem. Int. Ed. 57 (2018) 1888-1892.
- [9] R. M Zhu, J. W Ding, J. P Yang, et al., ACS Appl. Mater. Interfaces 12 (2020) 25037–25041
- [10] Z. Huang, Z. X Yang, Z. Hussain, et al., Electrochim. Acta 330 (2020) 135335.
- [11] L. Zhang, T. Mi, M.A. Ziaee, et al., J. Mater. Chem. A 6 (2018) 1639-1647.